

Poly lactide-Pine Woodflour Composites

Srikanth Pilla, Shaoqin (Sarah) Gong, Eric O'Neill,
Roger M. Rowell, and A. M. Krzysik

Abstract

Biobased and biodegradable polylactide (PLA)-pine wood flour (PWF) composites were investigated as a means to reduce the overall material cost and tailor material properties. The composites were prepared using a Kinetic-mixer and an injection molding machine. The tensile modulus of the PLA-PWF composites increased with the PWF content whereas the toughness and strain-at-break decreased. The tensile strength remained the same irrespective of the PWF content (up to 40%). The storage modulus increased with the PWF content. Additionally, composites containing PWF treated with silane showed higher storage modulus than those without silane treatment. The area integration underneath the $\tan \delta$ peaks decreased with increasing PWF, indicating that the PLA-PWF

composites exhibited more elastic behavior with increasing PWF. The degree of crystallinity of the PLA-PWF composites increased significantly with the PWF content. Furthermore, the treatment of PWF with silane was found to have a positive effect on its nucleating ability, as treated PLA-PWF composites showed higher crystallinity compared with non-treated counterparts. The morphology of the fracture surfaces were studied using a scanning electron microscope. Finally, a Halpin-Tsai analytical model to predict Young's modulus of PLA-PWF composites has been presented to compare the theoretical results with that of experimental ones.

Introduction

Plastics are one of the most highly valued materials mainly because of their extraordinary versatility and low cost (Stevens 2002). Their usage span a wide range of applications, such as packaging, structural (building materials), transportation, electrical components, biomedical, and consumer products. The increased use of plastics has become a significant concern because of its negative impact on the environment; specifically, the sources from which plastics are derived and their biodegradability. Almost all plastics are made from petroleum and its allied components. These natural resources take millions of years to form and are finite in quantity. In addition, plastics derived from fossil resources are largely non-biodegradable. The increased use in plastics over the years has resulted in an increase in plastic waste (both managed waste and litter), which often is dumped as municipal solid waste. Plastic litter in the oceans is a major threat for birds, fish, and other sea life. The majority of plastic

Pilla:

Graduate Student

Gong:

Assistant Professor, Department of Mechanical Engineering, University of Wisconsin, Milwaukee, Wisconsin, USA

O'Neill:

Forest Products Technologist, USDA Forest Products Laboratory, Madison, Wisconsin, USA

Rowell:

Professor, Department of Biological Systems Engineering, University of Wisconsin, and Pioneering Scientist, USDA Forest Products Laboratory, Madison, Wisconsin, USA

Krzysik:

Forest Products Technologist, USDA Forest Products Laboratory, Madison, Wisconsin, USA

waste today is reused via recycling; however, this reuse strategy has many limitations. Recycled plastics do not possess the same properties as their virgin counterparts (the properties deteriorate while recycling) and cannot be used in similar applications. Thus, there is an immediate need to look for alternative energy resources, and this has predominantly shifted the attention of many researchers toward biobased plastics. Biobased plastics are sustainable, largely biodegradable, and biocompatible (Gross and Kalra 2002, Bastioli 2001, Leaversuch 2002). They reduce our dependency on depleting fossil fuels and are CO₂ neutral. One of the most promising biobased polymers is poly(lactide) (PLA), which is made from agricultural products and is readily biodegradable. PLA, though discovered in 1890s, is finding an edge in this new era of science and will soon replace many commodity plastics because of its biodegradability property and biobased nature.

PLA is linear aliphatic thermoplastic polyester made from lactic acid (Carlotta 2001) (α -hydroxy acid). First, lactic acid is produced by the bacterial fermentation of corn, sugar cane, sugar beet, etc. Then it is oligomerized and finally dimerized, catalytically, to make lactide. This lactide monomer is polymerized using ring-opening polymerization to make high molecular weight PLA (Drumright et al. 2000, Lunt 1998). PLA has high modulus, reasonable strength, excellent flavor and aroma barrier capability, good heat sealability, and can be readily fabricated, thereby making it one of the most promising bio-polymers for varied applications (Fang and Hanna 1999). As such, PLA can become one of the most preferred commodity plastics in the future. Despite these desirable features, several drawbacks tend to limit its widespread applicability such as high cost, brittleness, and narrow processing windows. Polymer composites offer a convenient approach to tailor the materials cost and engineer the material properties.

Eco-friendly bio-composites, comprised of natural fibers and biobased plastics (polymers), are of great importance to the material world, not only as a feasible solution to growing environmental threats, but also as a sustainable solution to the uncertainty of the world's petroleum supply (Mohanty et al. 2002). Natural fibers have several advantages over traditional inorganic fillers, including renewable nature, a non-food agricultural-based economy, low cost, low density, low energy consumption, high specific strength and stiffness, CO₂ sequestration, biodegradability, and less wear on machinery (Mohanty et al. 2002, Samir et al. 2005). Mohanty et al. (2000) reviewed such composites and presented several different reinforcing bio-fibers and biodegradable polymers by analyzing the structure-

property relationship. They also showed how the properties of these composites vary with different fiber surface treatments. A number of other studies on bio-composites were discussed in the literature (Baillie 2004, Wool and Sun 2005).

Of the many types of natural fillers, wood flour (WF) has attracted much study (Gernandes et al. 2004, Qiu 2003) because it offers significant cost-reduction as well as ease in processing. WF has been used as filler material in a variety of polymers for property enhancement and reducing costs (Gernandes et al. 2004, Qiu 2003). Liber-Knec et al. (2006) investigated the mechanical properties of polypropylene (PP)-WF composites. The size and percentage of WF in the PP matrix were varied. They concluded that the addition of WF to PP enhanced the mechanical properties of PP. A similar study conducted by Ichazo et al. (2006) on natural rubber-based WF composites revealed that the addition of WF to natural rubber increased scorch time and curing time and caused improvement in modulus at 300 percent strain and in-tear properties; however, it decreased the tensile strength and elongation-at-break. Nonetheless, different percentages and sizes of WF were found to have different effects on the properties of their composites. Although good improvement in properties was found, there was some decline in strength and elongation-at-break, which may result from weak interfacial bonding between the filler (WF) and polymer, as both have a contrasting chemical and physical nature. Lee and Ohkita (2003) studied the effect of PCL-grafted-maleic anhydride (PCL-g-MA) compatibilizer on the properties of polycaprolactone (PCL) and polybutylenesuccinate-butylene carbonate (PBSC) based WF composites. They prepared samples with and without the compatibilizer and tested them for various mechanical and thermal properties. They found that tensile properties such as tensile strength, modulus, and elongation-at-break are higher in the samples that consist of PCL-g-MA compatibilizer than the ones that did not. This enhancement may result from the modification of the chemical nature of the filler for good adhesion with the polymer. This leads us to an important part of the research in which the addition of a suitable coupling agent will further increase the properties of WF composites compared with those that do not consist of the coupling agent. Many investigations, reported in the literature (Wu 2004, Li and Yan 2007, Jaing and Kamdem 2004, Shah et al. 2005), have been conducted in this area with a goal of improving interfacial bonding. Of all of the coupling agents mentioned in the literature, the one that is of interest in the present study is silane, which proved to provide good adhesion at the

interface of the WF and the polymer (Kokta et al. 1989, Raj et al. 1989, Kuan et al. 2003).

As the products made by these WF composites are used in variety of applications, it is also important to understand the behavior of WF composites in different weather conditions. An investigation conducted by Stark (2001) and Stark et al. (2004) on WF-filled PP and WF-high-density polyethylene (HDPE) composites, respectively, address this issue in which they fabricated samples using three methods: injection molded, extruded, and extruded and planed. Then they characterized them using Fourier transform infrared (FTIR) spectroscopy. The high processing pressures, to which the injection molded samples were subjected, resulted in a composite with higher density compared with the extruded and planed methods. With an improvement of the interfacial quality of WF and polymer, the high density can enhance the strength of injection molded samples compared with that of extruded and planed composites. In addition, when tested for weathering conditions for 3,000 hours, the injection molded samples retained higher flexural modulus of elasticity (MOE) and strength properties compared with the extruded and planed samples. In fact, the extruded and planed samples lost a larger percentage of their total mechanical properties during the first 1,000 hours of exposure. This is due to the exposure of the surface of the extruded and planed samples to moisture that resulted in loss of properties. The planed samples have a higher ability for moisture absorption due to strong hydrophilic wood content at the surface.

Thus, Stark (2001) and Stark et al. (2004) concluded that of the three fabrication processes, injection molded samples are best due to their superior properties and applications. The problem of moisture absorption deteriorating the properties of the WF composites was addressed by Mishra and Verma (2006), who have shown that by using a suitable compatibilizer, the absorption ability which occurs mainly because of the hydrophilic nature of the WF was reduced. The WFs hydrophilicity can be reduced when the WF is coated with a suitable compatibilizer (maleic anhydride in this case), thereby reducing the water (or moisture) absorption. This occurs mainly because of the ester linkages or bond formation of the WF with maleic anhydride, which further causes good adhesion between the filler and matrix by the formation of a hydrogen or chemical bond. Thus, the addition of a compatibilizer not only improves the mechanical properties as discussed previously, but also reduces the water absorption ability of the overall composite.

In addition to the static mechanical properties, researchers also are interested in the analysis of the dy-

namic mechanical (DMA) properties of polymers and their composites, as polymers with their natural ability of viscoelasticity tend to show variation in these properties with the addition of fillers and coupling agents. Ge et al. (2006) conducted a study on the DMA properties of poly (propylene carbonate) (PPC) based biodegradable composites. The storage modulus increased with increasing WF content, which is in agreement with their tensile modulus results. The glass transition temperature (T_g) (of PPC) obtained by the $\tan \delta$ peak was seen to shift to a higher value with the addition of WF. This increment in T_g , however, did not vary with WF content. A similar study by Ichazo et al. (2006) on natural rubber-wood flour composites inferred the same conclusion that the addition of WF shifted the $\tan \delta$ peak, thereby increasing the T_g . This can be attributed mainly due to the restriction caused on the mobility of polymer chains by the filler particles. On the other hand, Nenkova et al. (2006) investigated PP-WF composites and found a contrasting result that the addition of WF did not have a significant influence on the T_g of the polymer matrix; however, maleic anhydride- (MA) treated WF enhanced the amplitude of the $\tan \delta$ peaks, thereby confirming the chemical interaction of MA (coupling agent) with some components of WF. Additionally, there are numerous studies on non-WF-based bio-composites which showed that adding filler would increase the storage modulus significantly in line with tensile modulus. Though a comprehensive literature study on such composites is beyond the scope of this paper, they can be found in the public domain.

The addition of WF to polymers not only affects the mechanical properties but also the thermal properties, including crystallization behavior. Such properties can be investigated using differential scanning calorimetry (DSC). Several DSC studies on PLA and its composites were reported (Liu et al. 2001, Fischer et al. 1973, Mathew 2006). Mathew et al. (2005) have studied the effect of cellulose materials on the mechanical properties of PLA. They inferred that in a crystalline polymer matrix, the presence of fibers tends to influence the microstructure at the interface and thus the overall composite mechanical properties. The crystallinity of a polymeric system will depend on many factors such as the processing conditions (e.g., the heating-cooling cycles that the material passes through during extrusion and injection molding steps, especially the processing parameters such as the cooling rate and the crystallization temperature), nucleation density, and annealing time (Shulz et al. 1996). Of the different factors studied, Mathew et al. (2006) concluded that it is the surface topography of the fiber but not the chemical composition that plays a decisive role

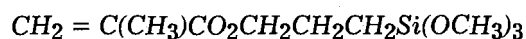
in crystallinity development. Eichhorn et al. (2001), however, have suggested that in the case of cellulose reinforcements, the presence of lignin is known to affect the ability of the fibers to act as the nucleating agent. Other studies conducted by Serizawa et al. (2006) and Qiu et al. (2003) also drew the same conclusion that the addition of cellulose-based natural fibers increases the crystallinity of the polymer (PLA in this case) as the fillers act as nucleating agents for the crystallization of the polymers. Thus, it is important to study the crystallization of polymer-filled composites to understand the effect of the fillers on the crystallinity of polymers.

In this study, we compounded the PLA-pine wood flour (PWF) composites with different PWF loading levels via a kinetic-mixer (K-mixer) and prepared the testing specimens via an injection molding machine. Specimens were prepared with and without treating the PWF with a coupling agent, silane. Various properties such as mechanical (static and dynamic) and thermal were compared. The static mechanical properties reported in this paper are tensile modulus, tensile strength, fracture toughness, and strain-at-break, and the dynamic mechanical properties reported are storage modulus and $\tan \delta$. The crystallization behavior was investigated using DSC. The morphologies of the fractured specimens captured using a scanning electron microscope were also investigated. Finally, an analytical model to predict the modulus of the composite system, developed by Halpin and Tsai (1967), has been presented and was compared with the theoretical and experimental results.

Experimental Section

Materials

PLA (NatureWorks™ PLA 3001D) in pellet form was obtained from Natureworks® LLC, Minnetonka, Minnesota. It has a specific gravity of 1.24 and a melt flow index around 15 g/10 min. (190°C/2.16 Kg). Its Tg is 68°C to 75°C and its melting temperature is 167°C. PWF (40 mesh/ 425 microns) was supplied by American Wood Fibers, Inc., Schofield, Wisconsin. The properties of PWF are presented in Table 1. GE Silicones - Silquest A-174® silane (gamma-Methacryloxypropyltrimethoxysilane), obtained from Witco Corporation, was used as the coupling agent. The chemical formula for silane is:



Methods

Processing PLA with PWF

An injection molding machine (Cincinnati Milacron Cmac Vsx 33-ton) was used to mold the tensile test

Table 1. ~ Pine woodfour properties.

Property	Value
Moisture content	Max 8%
Typical bulk density (pcf)	13
Typical acidity (pH)	4.7
Typical specific gravity	0.4
Typical ash content	0.5%

samples. Prior to processing, both PLA and PWF were dried in an oven at 55°C and ~105°C, respectively, to remove any moisture that had been absorbed during storage. The PWF was dried at a higher temperature to speed up the process. The dried samples were tested for moisture percentage using a moisture analyzer (Denver Instruments IR-200). If the moisture content was found to be too high (> 1%), additional drying was performed before further processing continued. A kinetic mixer (K-mixer) (Vanzetti Systems Series 3009) was used to blend PLA and PWF. First, the PWF was fed into the K-mixer and a few drops of silane (as per the percentage) were added. The silane percentage employed in this study is a percentage relative to the PWF content in the formulation; thus, the higher the PWF content, the higher the silane content. The K-mixer was turned on and once the rpm of the rotary chamber (mixing chamber) reached 5,000, it was switched off. This dispersed the silane within the PWF. Then, PLA in pellet (weighed for appropriate proportion) form was added to the mixing chamber and the machine was turned on again to raise the rpm to 5,000. This increased the temperature inside the chamber and as the four blades present inside the mixing chamber rotated at the set rpm, friction was generated that melted the polymer. Once melted, mixing with PWF (coated with silane) took place, and, as the temperature increased to a preset value (~400°F), the chamber door opened and a compounded semi-liquid mix was dumped into the basket located below. The semi-liquid mix was then quickly placed between two steel sheets that were inserted in a hydraulic press (Williams, White & Company). A force of nearly 900 psi was exerted to the polymer blend to give a thin "pancake" of the compound. The pancake was given 2 to 3 minutes to cool under the exerted force to avoid any warping. The pancakes must be granulated to feed into the injection molding machine. A granulator (Ball & Jewell Granulators Model# BP-68-SCS) was used to make granules of the compounded pancakes. The machine has three spinning blades that chop the pancakes into pieces until they are small enough to fit through a 1/8th inch diameter screen. This provides a

usable size particle that can easily be injection molded. The final step in processing was to make tensile test specimens (ASTM D638) using an injection molding machine (Cincinnati Milacron Cmac Vsx 33-ton). The granules were dried once again to remove any moisture that had been absorbed during the blending, pressing, and granulating process. This dry material was then fed into the hopper of the injection molding machine. The molder was run via specifications of the PLA. The following temperatures were set at respective zones: 395°F near the feeder, 400°F in the middle zone(s), and 405°F at the injection tip. While operating, great care must be taken to prevent the PLA from staying in the barrel of the injection molder at these temperatures for long because the material quickly degrades. A variable pack/hold pressure of 700 to 1,000 psi was used depending on the percent weight percentage of the PWF (700 psi for 20% and up to 1,000 psi for 40%). A packhold time of 15 seconds also was used to ensure maximum material in the mold. Since PLA has a low T_g, a mold temperature of 67°F was maintained to allow adequate freezing in the allotted cooling time. A cooling time of 40 seconds per part was provided to ensure the part did not break upon die separation. Samples were prepared and are listed in Table 2.

Tensile testing

The static tensile properties (modulus, strength, toughness, elongation-at-break) were measured at room temperature (~25°C) and atmospheric conditions (relative humidity [RH] of ~50% ± 5%) with a 5 kN load cell on an Instron Model 5566 tensile tester. The crosshead speed was set at 0.2 in/min. The extensometer used was an MTS 634.31E-24 with a 1-inch gauge length. All of the tests were carried out according to the ASTM standard; five specimens of each sample were tested and the average results were reported. All of the samples were tested after having been subjected to room temperature and atmospheric conditions for several weeks.

DMA

The dynamic mechanical spectra of the different specimens, cut from injection molded samples, were

obtained using a dynamic mechanical spectrometer (TA instrument, model DMA Q800), which was equipped with a dual cantilever mode. The specimens were tested in a single-cantilever mode and under liquid nitrogen atmosphere. They were heated at a rate of 3°C/min. from 0°C to 85°C with a frequency of 1 Hz and strain of 0.02 percent, which is in the linear viscoelastic region as determined by a strain sweep.

Scanning electron microscopy

Fractured surfaces from the tensile tests were examined using scanning electron microscopy (SEM) (Hitachi S-570) operated at 10KV All specimens were sputter coated with a thin layer of gold (~20 nm) prior to examination. The comparison between micrographs of different specimens was made at the same level of magnification.

DSC

The DSC analysis was conducted on a sample sliced from injection molded specimens using a differential scanning calorimeter (TA Instruments, Auto DSC-Q20). The sample was first heated from 40° to 180°C, kept isothermal for 3 minutes, quenched to 0°C, and finally reheated to 200°C. The ramp speed in all of the heating-cooling processes was 10°C/min.

Results and Discussion

Structure of PWF

The composition of the PWF reinforcement is presented in Table 3, which shows that the nature of the material is complex, i.e., consisting of many constituents. The majority portion is composed of hydrophilic cellulose and the remaining part, in which lignin dominates, corresponds to hydrophobic substances. The PWF used in this study does not possess a standard geometric pattern and dimension as in the case of glass or carbon fibers, which have relatively uniform shapes, i.e., a quasi-constant diameter. In fact, any WF particle can be classified as a bundle of cellulose fibrils connected by non-cellulose components, with aspect ratios no greater than 6-8 (Cunha et al. 2001). An SEM image of PWF used in this study is shown in **Figure 1**. As can be inferred from **Figure 1**, PWF does not have a fixed geometry and varies in length and diameter (l/d ratio: 3-5). The supplier reported WF size is 40 mesh/425 microns. It has very low thermal conductivity due to the tubular structure, which provides excellent low thermal conductivity (0.05–0.07 W • m⁻¹ • K⁻¹) (Grobe 1989). Also, the rough surfaces seen on the outer structure of the PWF may benefit the interfacial adhesion provided an appropriate coupling agent is used.

Table 2. ~ List of processed materials.

Material
PLA
20% PWF-0% Silane
20% PWF-0.5% Silane
40% PWF-0% Silane
40% PWF-0.5% Silane

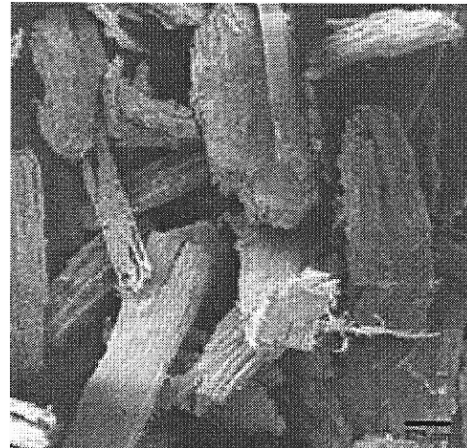
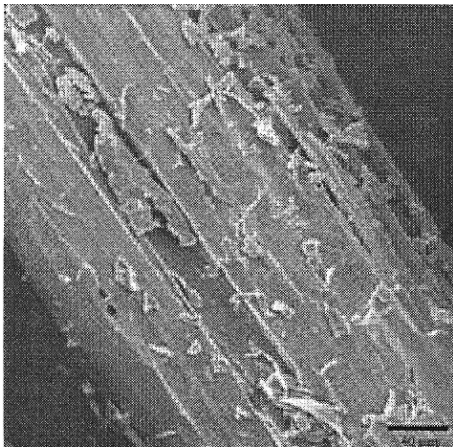


Figure 1. ~ SEM images of PWF at different magnifications: 40 μm (left) and 125 μm (right).

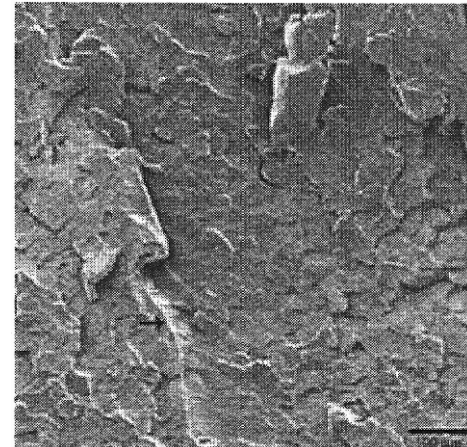
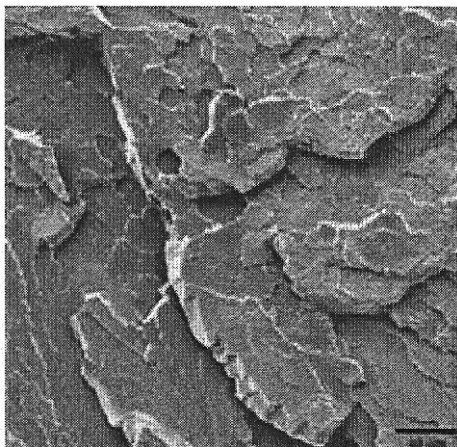


Figure 2. ~ SEM images of pure PLA at different magnifications: 40 μm (left) and 100 μm (right).

Table 3. ~ Composition of wood flour reinforcement (Cunha et al. 2001).

Ingredient	Percentage
Cellulose	42
Lignin	30
Galactoglucomannan	20
Xylan	8

Morphology of the Fractured Surface

The morphology of the fractured surface of the injection molded specimen resulting from the tensile testing experiments was investigated using SEM to understand the fracture behavior of PLA-PWF composites. It was assumed that the samples would fracture at the weakest point in the sample. For the purpose of recognizing the individual phases within the composite, SEM images for PWF (**Fig. 1**) and pure PLA (**Fig. 2**) were also scanned.

Figures 3 and 4 show the SEM images of fractured surfaces of the composite specimens at different PWF levels treated with and without silane, respectively. The effect of silane could not be predominantly identified in the SEM images; however, the increased PWF content can be well seen. A comparison of the images at the same magnification reveals that PWF is much more densely packed in higher percentage samples. As quoted in Chapter 1 of Agarwal and Broutman (1990), the more the percentage of filler, the stiffer the composite will be. Thus, the dense sample, 40 percent PWF composite, is believed to be stiffer than the rest, which has been confirmed in the tensile test results discussed in the subsequent section. By examining the images that give an understanding of the type of fracture that took place, we can infer that PLA showed a smooth fracture surface without obvious plastic deformation. Similar morphology can be observed in composite specimens (20% and 40% PWF), demonstrating that brittleness predominates the fracture mode. As

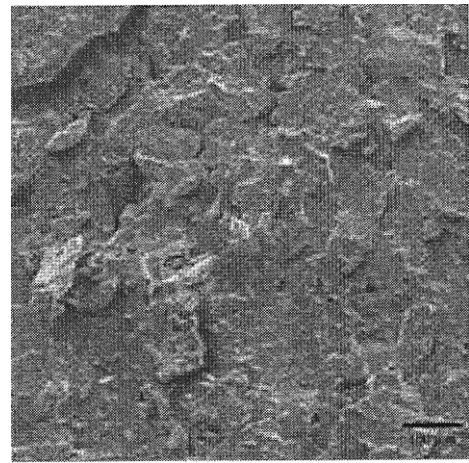
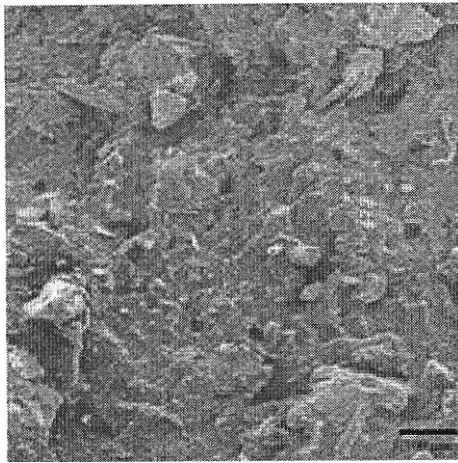


Figure 3. ~ SEM images of PLA-20% PWF: 100 μm (left, 0% silane) and 100 μm (right, 0.5% silane).

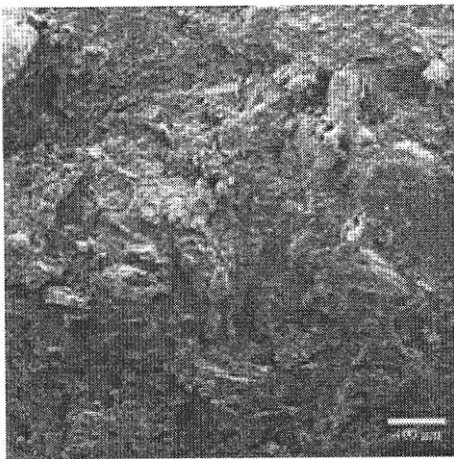


Figure 4. ~ SEM images of PLA-40% PWF: 100 μm (left, 0% silane) and 100 μm (right, 0.5% silane).

shown in **Figures 3 and 4**, an accurate distinction cannot be made between PLA and WF, indicating that good adhesion exists between the two. This was confirmed later in the tensile test results discussed in the subsequent section, in which the strength of the composite remained the same regardless of the PWF loading, which generally is not the case in PLA-WF composites (Zuiderduin et al. 2003). When the PWF content is higher, it is evident that the density of PWF increases within the composite sample. A high PWF loading level could hinder the deformability of the polymer matrix (PLA in this case) due to the restriction offered by the rigid filler particles, thereby decreasing the strain-at-break percentage (Nunez 2003).

Tensile Properties

Tensile tests (according to ASTM D638) were performed on injection molded PLA-PWF specimens and properties such as energy-to-break (toughness), strain-at-break, modulus, and strength were computed.

All of the specimens tended to follow the brittle fracture mode as evident from the SEM images and stress-strain curves (**Fig. 5**). The brittleness increased with PWF content. An important feature associated with brittleness is necking before fracture, which is not seen in any PWF-filled specimen (**Fig. 5**). Only PLA exhibited some necking in the stress-strain curve, demonstrating that it is less brittle compared with PWF-filled samples and has undergone stress-whitening during the tensile test. The stress-whitening phenomenon observed in the pure PLA samples is caused by crazing. Crazing is a phenomenon that frequently precedes fracture in some thermoplastic polymers (Anderson 1995, Kinloch and Young 1983). It is a dilative process and is a feature of localized plastic deformation. Crazing occurs in regions of high hydrostatic tension or in regions of much localized yielding, which leads to the formation of interpenetrating microvoids and small fibrils. If an applied tensile load is sufficient, these bridges elongate and break, causing the

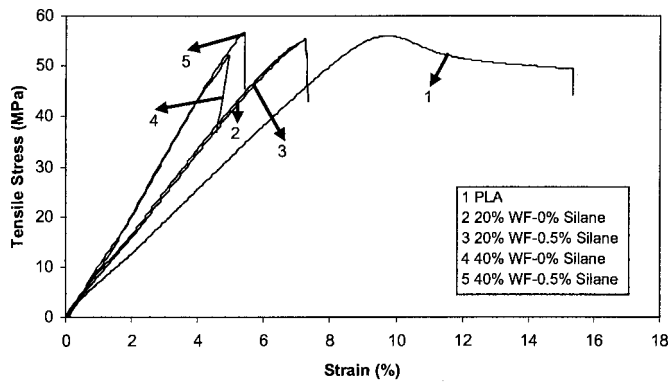


Figure 5. ~ Tensile stress-strain curves of PLA-PWF composites.

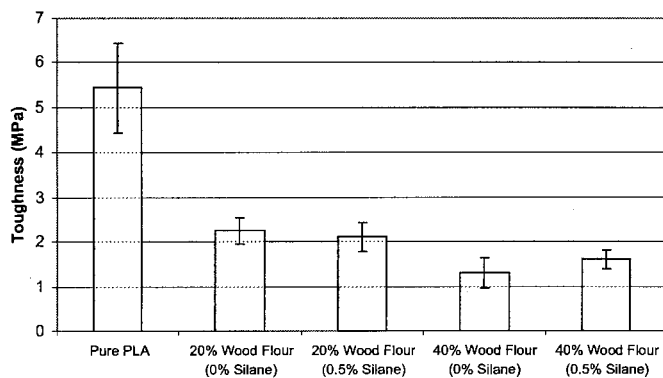


Figure 6. ~ Toughness of PLA-PWF composites.

micro voids to grow and coalesce; as micro voids coalesce, cracks begin to form. Unlike the PWF-filled composites, in the tensile tests, pure PLA yielded by crazing (indicated by an arrow in **Fig. 2**, right) under the test condition (crosshead speed 0.2 in./min., temperature 25°C). More crazes result in higher strain-at-break values and toughness (Anderson 1995). The crazes vanished when PWF was added to pure PLA, indicating that filled composites exhibit lower toughness. This has been confirmed by toughness results obtained by the tensile tests (**Fig. 6**) discussed later.

The brittleness of a material is often gauged using material properties such as toughness and strain-at-break. The toughness of the PWF-filled samples decreased significantly when compared to pure PLA (**Fig. 6**). Toughness, which is the energy to fracture per unit volume (Van Vlack) of the specimen, is obtained by integrating the area under the stress-strain curve (**Fig. 6**). The decrease in toughness is mainly due to the brittle nature of the PWF. Thus, the higher the PWF loading the lower the toughness (**Fig. 6**). Treatment of PWF with silane has shown to meagerly affect toughness. At 20 percent PWF content, it is negligible; but at a higher percentage, toughness increased. Thus it can

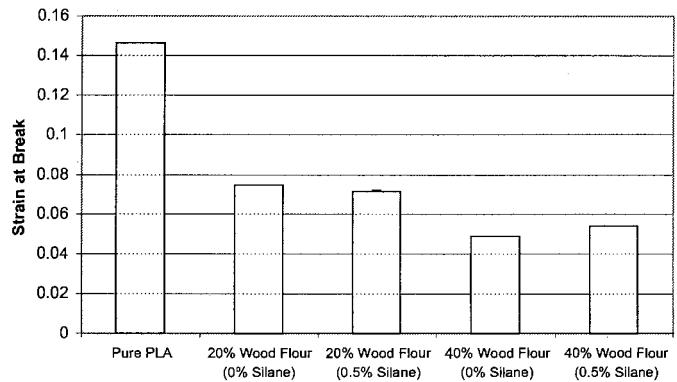


Figure 7. ~ Strain-at-break of PLA-PWF composites.

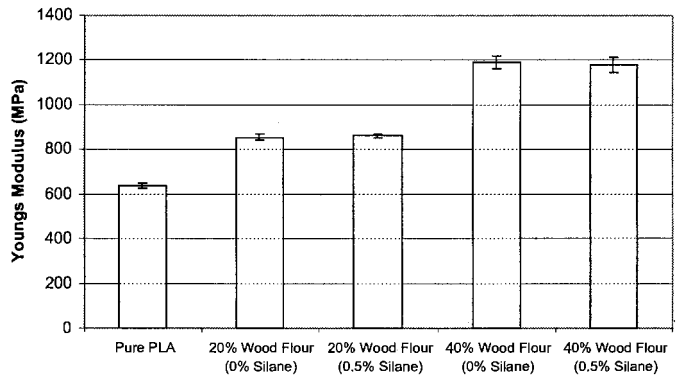


Figure 8. ~ Young's modulus of PLA-PWF composites.

be inferred that the addition of silane would increase the toughness properties (though not significantly) at higher PWF loading levels. This is an important feature as at higher WF loading levels, the composites tend to become more and more brittle which might hinder its usage in several important applications where toughness is an important criterion in addition to strength and stiffness. Strain-at-break is an important property that is defined by the tensile tests since it gives a good understanding about the deformability of the polymer matrix. **Figure 7** shows the strain-at-break percentages of the PLA-PWF composite at different PWF loading levels. As the Figure illustrates, the strain (%) decreased with increasing PWF content owing to decreased deformability of the matrix (PLA in this case) due to the restriction offered by the rigid filler particles. This can be well identified in the SEM images, which show much denser PWF in the composites at higher PWF loadings. The effect of silane on strain-at-break is similar to toughness as previously discussed, i.e., silane, increased the strain-at-break value at 40 percent PWF content, but had basically no effect at 20 percent PWF content.

The modulus of PLA increased with the PWF content (**Fig. 8**). The effect of silane cannot be seen clearly in this case; thus, it can be noted that it is more the

filler content than the coupling agent that plays a vital role in enhancing the tensile modulus of a composite. This increment in modulus is in agreement with the literature (Nunez et al. 2003) in which the reinforcement restrains the movement of the polymer chains, thereby increasing stiffness. As discussed in the morphology section, higher filler content showed a much higher density of PWF in the polymer that resulted in a stiffer composite. The tensile strength of filled composites generally is found to decline when compared with their virgin polymer (Zuiderduin et al. 2003). In this study, however, as can be seen from **Figure 9**, consistent strength was found for different levels of PWF. This can be attributed to the good interfacial adhesion between the PWF and PLA, which might result from the very nature (rough) of PWF as discussed previously and/or the coupling agent (silane). The effect of silane on the strength of PLA-PWF composites is similar to other tensile properties such as energy-to-break (toughness) and strain-at break, i.e., minimum or none at lower levels of PWF (20%) and reasonably significant at higher levels (40%). Thus, it can be concluded that the silane effect on tensile properties of PWF-filled composites is more prominent in higher PWF content specimens than their lower counterparts.

Halpin-Tsai Model for Young's Modulus

A wide variety of theoretical models (referred to here as 'model') exists to predict the elastic properties of conventional fiber composites in terms of the properties of the constituent materials (Chou 1992). In some special cases where specific fiber arrangements are considered, closed-form elastic solutions can be obtained. In this study, we considered Halpin and Tsai (1967) (H-T) empirical equations, which hold good for short fiber composites and when the fibers are randomly oriented in the polymer matrix.

Young's modulus, E , of a randomly oriented short fiber composite is given by Halpin-Tsai as:

$$E_r = \frac{3}{8}E_L + \frac{5}{8}E_T \quad [1]$$

where:

E_L and E_T are longitudinal and transverse moduli, given below:

$$E_L = E_m \left[\frac{1 + (2l/d)\eta_L V_f}{1 - \eta_L V_f} \right] \text{ and} \quad [2]$$

$$E_T = E_m \left[\frac{1 + 2\eta_T V_f}{1 - \eta_L V_f} \right]$$

The constants η_L and η_T are given as:

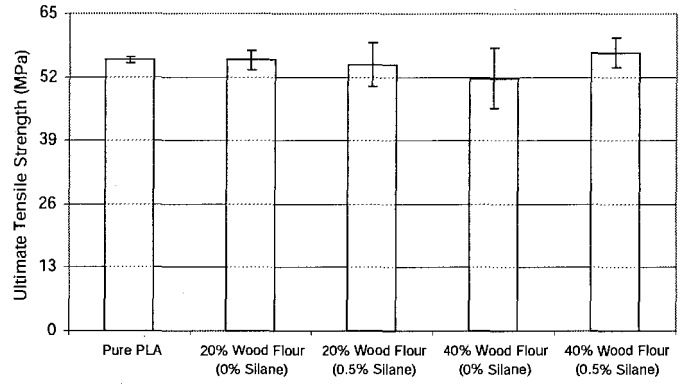


Figure 9. ~ Ultimate tensile strength of PLA-PWF composites.

$$\eta_L = \frac{(E_f / E_m) - 1}{(E_f / E_m) + (2l/d)} \text{ and}$$

$$\eta_T = \frac{(E_f / E_m) - 1}{(E_f / E_m) + 2} \quad [3]$$

In Equations **[1]**, **[2]**, and **[3]**:

E_f = Young's modulus of reinforcement (PWF),

E_m = Young's modulus of polymer (PLA),

V_f = volume fraction of reinforcement,

V_m = volume fraction of polymer i.e., $1 - V_f$ and

l/d = aspect ratio of reinforcement.

Figure 10 compares the model results predicted by Halpin-Tsai empirical relation for the modulus of the PLA-PWF composite with the experimental results obtained from tensile testing. The properties of PWF and PLA used in the H-T model (**Table 4**) are obtained from the literature (www.me.gatech.edu/jonathan.colton/me4793/natfiber.pdf) and experiments, respectively. Since no literature was found for 40 mesh PWF, properties of 30 mesh have been used in the model, which are believed to be close enough for computation and comparison. As the Figure shows, Young's modulus increases with PWF content. Experimental results with and without silane have been furnished. Though the model and experimental results do not coincide, they show a similar trend. The observed mismatch between the theoretical and experimental results is due to the following factors (Shi et al. 2004, Shi et al. 2004, Fisher 2003):

1. The model does not account for the interface between the filler and polymer.
2. The model does not consider the agglomeration, which generally is seen in filled composites due to the improper mixing of fillers and polymer.

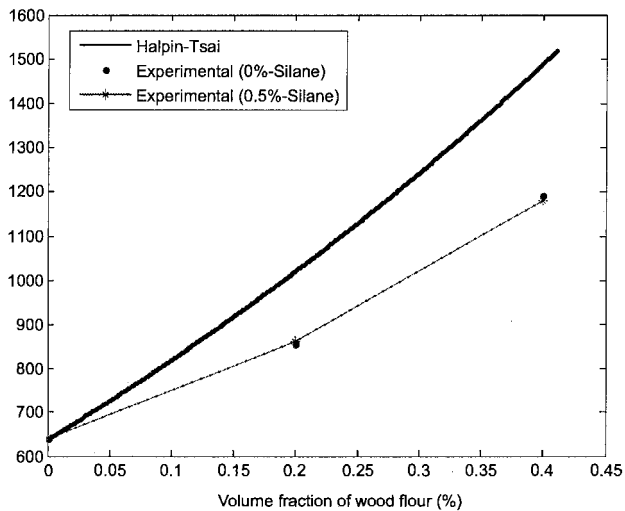


Figure 10. ~ Comparison of Halpin-Tsai (Halpin and Tsai 1967) and experimental results for Young's modulus of PLA-PWF composite.

Table 4. ~ Properties of constituent materials of the composite used in Halpin-Tsai model.

Property	Value
E_f	5500 MPa
E_m	638.87 MPa
V_f	0 to 0.5
l/d	4

3. Though the measured experimental properties vary between one replica to another, such variability is not being considered in the model.

Additionally, as previously stated, there was no specific data available for the 40 mesh PWF employed for this study, which required us to consider properties of 30 mesh PWF in the model. Thus, the model can be developed further to minimize the mismatch between the experimental and theoretical results by accounting for the first three conditions and by obtaining sufficient data for the 40 mesh PWF. Though literature is available in the public domain that has accounted for interface and statistical variations in the prediction of modulus of fiber composites, a comprehensive work on these aspects is beyond the scope of this paper.

Dynamic Mechanical Analysis

The viscoelastic properties of the PLA-PWF composites were studied using DMA. A general declining trend of storage modulus (Fig. 11) for all of the curves is observed when the specimens go through higher temperatures with the most rapid reduction occurring at $\sim 69^\circ\text{C}$, corresponding to the T_g of PLA. In general, storage modulus appeared to increase with increasing

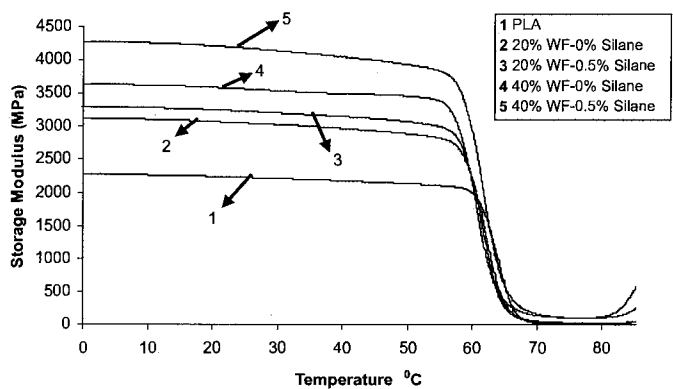


Figure 11. ~ Storage modulus of PLA-PWF composites as a function of temperature.

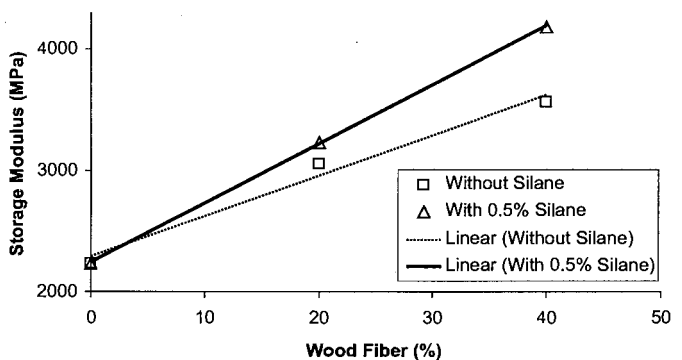


Figure 12. ~ Comparison of storage modulus (at 25°C) of PLA-PWF composite at different PWF ratios.

PWF content, which is in agreement with the tensile modulus measurement (Fig. 8). Unlike other properties, the effect of silane clearly is visible in the case of dynamic viscoelastic properties of PLA-PWF composites. The addition of a small amount of silane (0.5% of the PWF) has significantly improved the storage modulus of the composites at the same PWF loading level. This trend is in accordance with studies from the literature (Nenkova et al. 2006, Behzad et al. 2004). As shown in Figure 11, the storage modulus of the 20 percent and 40 percent PWF sample with 0.5 percent silane is higher than the 20 percent and 40 percent PWF sample with 0 percent silane, respectively. This explains the reason for treating the PWF with silane. Figure 12 shows such a trend in which the storage modulus, at 25°C , of respective specimens has been plotted against the PWF content. The linear curve fit best interpolates the experimental data indicating that the storage modulus increases linearly with PWF percentage (both treated and non-treated). The loss factor ($\tan \delta$) is shown in Figure 13. As can be seen in the Figure, the PWF content has little or no effect on

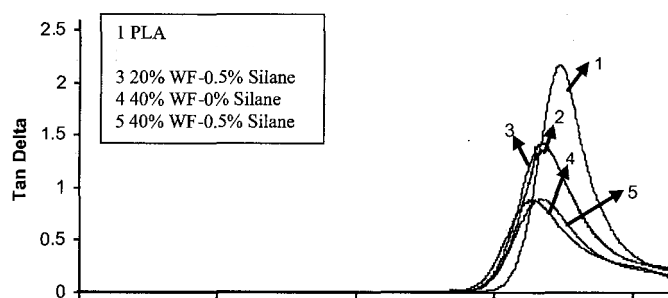


Figure 13. ~ Loss factor ($\tan \delta$ peak) of PLA-PWF composites as a function of temperature.

the peak temperatures, representing T_g . In fact, the peak broadened and shifted toward the left by a slight margin. This is in agreement with that reported in the literature (Nenkova et al. 2006). The area integration under the $\tan \delta$ curve decreased with increasing PWF content, indicating that the PLA-PWF composites exhibited more elastic behavior with increasing PWF, which is in accordance with the tensile test parameters. The meager effect of PWF content on the T_g s of the PLA-PWF composites are reported in **Table 5**.

DSC

The crystallization effects were studied using DSC. **Figure 14** shows the thermograms obtained from the second heating cycle; **Table 6** shows the numerical values of temperature and enthalpy obtained from the first cooling and second heating cycles and crystallinity for the PLA-PWF composites with different PWF and silane percentages. The addition of PWF induced a very slight reduction in the melting temperature of PLA. The largest decrease in T_m that occurred with the PLA-40 wt%PWF composite is approximately 2°C.

The cold crystallization temperature was decreased by about 14°C for a PLA-20%PWF (non-treated with silane) composite specimen when compared with pure PLA. In fact, the cold crystallization peak vanished

Table 5. ~ T_g s of the PLA and PLA-pine wood fiber composites.

Material	T_g (°C)
PLA	69.36
20% PWF-0%Silane	67.40
20% PWF-0.5%Silane	66.75
40%PWF-0% Silane	65.57
40% PWF-0.5%Silane	66.76

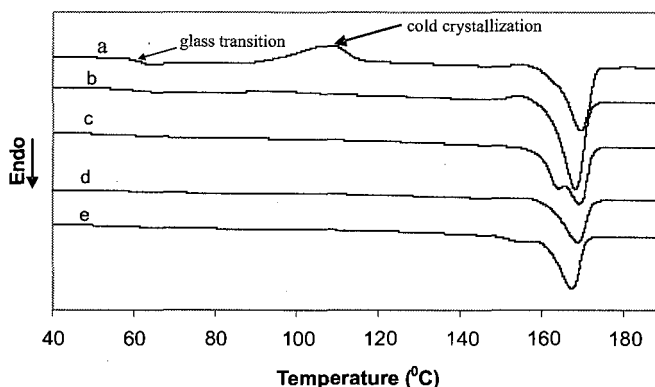


Figure 14. ~ Melting curves of PLA-PWF composites. Data obtained from the second heating run. (a) PLA; (b) PLA/20%PWF-0%Silane; (c) PLA/20%PWF-0.5%Silane; (d) PLA/40% PWF-0% Silane; and (e) PLA/40% PWF-0.5% Silane.

completely for each of the other three PLA-PWF samples, namely PLA-20%PWF (treated with silane) and PLA-40%PWF (treated and non-treated with silane) indicating that no additional amorphous region in those samples exists that has the ability to crystallize during the second heating process. Thus, all of the crystallization took place during the cooling process. These observations indicate that PWF, especially silane-treated PWF, acted effectively as a nucleating

Table 6. - Thermal characteristics of PLA and its composites.

PLA:PWF:Silane (%)	Cold-crystallization		Melting		Melting- crystallization temperature (°C)	Crystallinity (%)
	Temperature T_c (°C)	Enthalpy (J/g)	Temperature T_m (°C)	Enthalpy (J/g)		
100:0:0	108.71	25.02	169.70	37.10	92.43	13
80:20:0	94.73	4.059	168.52	32.72	95.78	38
79.5:20:0.5	--	--	169.59	37.51	111.48	50
60:40:0	--	--	169.09	24.62	94.60	44
59.5:40:0.5	--	--	167.48	28.37	98.15	51

agent for PLA crystallization during the cooling process.

The crystallinity of PLA is computed using Equation [4] (Fischer et al. 1973, Vasantakumari and Pennings 1983, Reinsch and Kelley 1997):

$$\chi_c (\% \text{ Crystallinity}) = \frac{\Delta H_m}{\Delta H_m^0} \times \frac{100}{w} \quad [4]$$

where:

$$\Delta H_m^0 = 93.7 \text{ J/g}$$

w - weight fraction of PLA in the sample

where:

ΔH_m = is the enthalpy for melting,

ΔH_m^0 = the enthalpy of melting for a 100% crystalline PLA sample, and

w = the weight fraction of PLA in the sample.

To determine the crystallinity of the sample, the extra heat absorbed by the crystallites formed during heating (i.e., cold crystallization) had to be subtracted from the total endothermic heat flow due to the melting of the whole crystallites (Nam et al. 2003). As shown in Table 6, the crystallinity of PLA increased from 13 to 51 percent (almost three times higher) when 40 percent of PWF treated with silane was added. Also it can be inferred from Table 6 that the crystallinity of PLA was higher for samples with the same PWF content but treated with silane. For instance, the crystallinity of PLA-20%PWF composites treated with silane is 12 percent higher than that of PLA-20%PWF composites without any silane treatment. Similarly, the crystallinity of PLA-40%PWF composites treated with silane is 7 percent higher than that of PLA-40%PWF composites without any silane treatment. In fact, the crystallinity of the PLA-20% PWF composite treated with silane (50%) is 6 percent more than that of the PLA-40% PWF composite without any treatment (44%). This indicates that silane played an important role in improving the crystallinity of PLA-PWF composites. This is in agreement with that reported in the literature (Eichhorn et al. 2001), in which the surface chemistry of fibers is the governing factor for the crystal formation in PLA-based composites. Thus, it can be concluded that the addition of PWF increases the crystallinity by acting as a nucleating agent; however, a treatment with a coupling agent such as silane further enhances crystallinity.

Conclusions

PLA-PWF composites were prepared by K-mixer and an injection molding machine. A morphological study of PWF showed a rough surface on the outer

structure that was believed to provide good interfacial adhesion. Similar studies on PLA-PWF composites revealed good adhesion between PLA and PWF and good dispersion of PWF in the polymer. Pure PLA yielded by crazing as is evidenced from the stress-whitening phenomenon and the SEM micrograph; however, crazing was not observed in the PLA-PWF composites.

The addition of PWF increased the modulus but decreased the toughness and strain-at-break; strength remained the same. The effect of silane on the tensile properties became discernable at a higher PWF loading level (i.e., 40%). The theoretical Young's modulus predicted by Halpin-Tsai empirical relation was found to increase with increasing PWF content; however, some mismatch exists between the theoretical and experimental results due to the reasons discussed previously.

The storage modulus of the PLA-PWF composites was found to increase with increasing PWF content. Further the effect of silane was clearly visible as the specimens with silane generally showed higher values of storage modulus than their non-silane counterparts. The addition of PWF to PLA was found to have no or less effect on the Tgs taken from the peak values in the tan δ curves.

The addition of PWF induced a slight reduction in the melting temperature of the composites. The cold crystallization peak decreased with addition of 20 percent PWF non-treated with silane and eventually disappeared for all other PLA-PWF composites investigated. The crystallinity of PLA was enhanced significantly (up to three times higher) by the addition of PWF. Additionally, it was found that the crystallinity was affected by silane. PWFs treated with silane showed higher nucleating ability than non-treated PWFs. The silane-treated PWFs, when compared to non-treated PWFs, increased the crystallinity of the PLA-PWF composites about 12 percent and 7 percent at 20 percent and 40 percent PWF loading level, respectively.

Acknowledgments

The financial support from National Science Foundation (NSF DMI-0544729) and Wisconsin Department of Agriculture, Trade and Consumer Protection is gratefully acknowledged.

Literature Cited

- Agarwal, B. and L. Broutman. 1990. Analysis and Performance of Fiber Composites. John Wiley & Sons Inc., NY.
- Anderson, T.L. 1995. Fracture Mechanics, 2nd ed. CRC Press, Boca Raton, FL. pp. 34,322,377.
- Baillie, C., Ed. 2004. Green Composites: Polymer Composites and the Environment. Woodhead Publishing Ltd. ISBN:1855737396.

- Bastioli, C. 2001. *Starch/Staerke*. 53(8): 351-355.
- Behzad, M., M. Tajvidi, G. Ebrahimi, and R.H. Falk. 2004. *IJE Transactions B: Applications*. 17(1): 95-104.
- Chou, T-W. 1992. *Microstructural Design of Fibercomposite*. Cambridge Univ. Press.
- Cunha, A.M., Z.Q. Liu, Y. Feng, X-S. Yi, and C.A. Bernardo. 2001. *J. Mat. Sci*. 36: 4903-4909.
- Drumright, R.E., P.R. Gruber, and D.E. Henton. 2000. *Adv. Mat*. 12(23): 1841-1846.
- Eichhorn, S.J., C.A. Baillie, N. Zafeiropoulos, L.Y. Mwaikambo, M.P. Ansell, A. Dufresne, K.M. Entwistle, P.J. Herrera-Franco, G.C. Escamilla, L. Groom, M. Hughes, C. Hill, T.G. Rials, and P.M. Wild. 2001. *J. Mat. Sci*. 36: 2107-2131.
- Fang, Q. and M.A. Hanna. 1999. *Ind. Cor. and Prod*. 10(1): 47-53.
- Fernandes, E.G., M. Pietrini, and E. Chiellini. 2004. *Biomacromolecules*. 5: 1200-1205.
- Fischer, E.W., H.J. Sterzel, and G. Wegner. 1973. *Kolloid-Z. Z. Polymere*. 251(11): 980-990.
- Fisher, ET., R.D. Bradshaw, and L.C. Brinson. 2003. *Comp. Sci. and Tech*. 63(11): 1689-1703.
- Garlotta, D. 2001. *J. Polym. and the Envi*. 9(2): 63-84.
- Ge, X.C., Q. Zhu, and Y.Z. Meng. 2006. *J. App. Polym. Sci*. 99: 782-787.
- Grobe, A. 1989. *Polymer Handbook*. John Wiley & Sons, Inc., NY.
- Gross, R.A. and B. Kalra. 2002. *Sci*. 297(5582): 803-807.
- Halpin, J.C. and S.W. Tsai. 1967. *U.S. Airforce Technical Report*. AFML TR, 67-423.
- Hristov, VN., M. Krumova, S. Vasileva, and G.H. Michler. 2004. *J. App. Polym. Sci*. 92: 1286-1292.
- Ichazo, M.N., C. Albano, J. Gonzalez, R. Perera, and M.V. Candal. 2001. *Comp. Struc*. 54: 207-214.
- Ichazo, M.N., M. Hernandez, C. Albano, and J. Gonzalez. 2006. *Macro. Sym*. 239: 192-200.
- Jaing, H. and D.P. Kamdem. 2004. *J.Vin. & Add. Techn*. 10(2): 70-78.
- Jiang, L., M.P. Wolcott, and J. Zhang. 2006. *Biomacromolecules*. 7: 199-207.
- Kinloch, A.J. and R.J. Young. 1983. *Fracture Behavior of Polymers*. Applied Sci. Publishers: London. pp. 132,147, 162.
- Kokta, B.V., R.G. Raj, and C. Daneault 1989. *Polym. Plas. Tech. Eng*. 28(3): 247-259.
- Krishnamurthi, B., S. Bharadwaj-Somaskandan, T. Sergeeva, and E Shutov. 2003. *Cell. Polym*. 22(6): 371-381.
- Kuan, C.F., H.C. Kuan, C.C.M. Ma, and C.M. Huang. 2006. *Composites Part-A*, 37(10): 1696-1707.
- Kuan, H.C., J. M. Huang, C.C.M. Ma, and EY. Wang. 2003. *Plas., Rub. and Comp*. 32(3): 122-126.
- Leaversuch, R. 2002. *Plas. Tech*. 48(9): 66-73.
- Lee, S-H. and T. Ohkita. 2003. *J. App. Polym. Sci*. 90: 1900-1905.
- Li, T. and N. Yan. 2007. *Comp. Part-A*. 38: 1-12.
- Liber-Knec, A., S. Kuciel, and W. Dziadur. 2006. *Polimery*. 51(7/8): 571-575.
- Lin, H.R., M.D. Shau, and Z.W. Chiou. 2001. *J. Polym. Res*. 8(4): 241-251.
- Lin, Q., X. Zhou, G. Dai, and Y. Bi. 2002. *J. App. Polym. Sci*. 85: 536-544.
- Liu, Z.Q., A.M. Cunha, X.S. Yi, and C.A. Bernardo. 2001. *J. Macro. Sci. - Phy*. 40B(3/4): 529-538.
- Lunt, J. 1998. *Polym. Deg. and Stab*. 59(1/3): 145-152.
- Mathew, A.P., K. Oksman, and M. Sain. 2005. *J. App. Polym. Sci*. 97(5): 2014-2025.
- Mathew, A.P., K. Oksman, and M. Sain. 2006. *J. App. Polym. Sci*. 101: 300-310.
- Mishra, S. and J. Verma. 2006. *J. App. Polym. Sci*. 101: 2530-2537.
- Mohanty, A.K., M. Misra, and L.T. Drazel. 2002. *J. Polym. and the Env*. 10(1/2): 19-26.
- Mohanty, A.K., M. Misra, and G. Hinrichsen. 2000. *Macro. Mat. and Eng*. 276-277(1): 1-24.
- Nam, J.Y., S.S. Ray, and M. Okamoto. 2003. *Macromolecules*. 36: 7126-7131.
- Nenkova, S., C.V. Dobrilova, M. Natov, S. Vasileva, and P. Velev. 2006. *Polym S. and Polym. Comp*. 14(2): 185-194.
- Nunez, A.J., P.C. Sturm, J.M. Kenny, M.I. Aranguren, N.E. Marcovich, and M.M. Reboredo. 2003. *J. App. Polym. Sci*. 88: 1420-1428.
- Oksman, K. and C. Clemons. 1986. *J. App. Polym. Sci*. 67: 1503-1513.
- Oksman, K. and H. Lindberg. 1998. *J. App. Polym. Sci*. 68: 1845-1855.
- Oksman, K., H. Lindberg, and A. Holmgren. 1998. *J. App. Polym. Res*. 69: 201-209.
- Oksman, K., M. Skrifvars, and J-E Selvin. 2003. *Comp. Sci. and Tech*. 63: 1317-1324.
- Pukanszky, B. 2005. *Euro. Polym. J*. 41(4): 645-662.
- Qiu, W., E Zhang, T. Endo, and T. Hirotsv. 2003. *J. App. Polym. Sci*. 87: 337-345.
- Raj, R.G., B.V. Kokta, D. Maldas, and C. Daneault. 1989. *J. App. Polym. Sci*. 37(4): 1089-1103.
- Reinsch, V.E. and S.S. Kelley. 1997. *J. App. Polym. Sci*. 64(9): 1785-1796.
- Samir, M.A.S.A., E Allioin, and A. Dufresne. 2005. *Biomacromolecules*. 6, 612-626.
- Serizawa, S., K. Inone, and M. Iji. 2006. *J. App. Polym. Sci*. 100:618-624.
- Shah, B.L., L.M. Matuana, and P.A. Heiden. 2005. *J. Vinyl and Add. Tech*. 11(4): 160-165.
- Shi, D.L., X.Q. Feng, Y. Huang, K.C. Hwang, and H. Gao. 2004. *J. Eng. Mat. and Tech*. 126: 250-257.
- Shi, D.L., X.Q. Feng, Y. Huang, and K.C. Hwang. 2004. *Key Eng. Mat*. pp. 261-263, 1487-1492.
- Shulz, E., G. Kalinka, and W. Auersch. 1996. *J. Macro. Sci. Part B: Physics*. 35(3/4): 527-546.
- Stark, N. 2001. *J. Thermo. Comp. Mat*. 14: 421-432.
- Stark, N.M., L.M. Matuana, and C.M. Clemons. 2004. *J. App. Polym. Sci*. 93: 1021-1030.
- Stevens, E.S. 2002. *Green Plastics: An introduction to the new science of biodegradable plastics*. Princeton Univ. Press.
- Tsuji, H. and Y. Ikada. 1995. *Polymer*. 36(14): 2709-2716.
- Tsuji, H. and Y. Ikada. 1996. *Polymer*. 37(4): 595-602.
- Van Vlack, L.H. *Elements of Materials Science and Engineering*, 6th ed. Addison-Wesley Publishing Co. p. 271.

- Vasanthakumari, R. and A.J. Pennings. 1983. *Polymer*. 24(2): 175-178.
- Vladkova, T.G., P.D. Dineff, and D.N. Gospodinova. 2004a. *J. App. Poly. Sci.* 91: 883-889.
- Vladkova, T.G., P.D. Dineff, and D.N. Gospodinova. 2004b. *J. App. Polym. Sci.* 92: 95-101.
- Vladkova, T.G., P.D. Dineff, D.N. Gospodinova, and I. Avramova. 2006. *J. App. Polym. Sci.* 101: 651-658.
- Vladkova, T.G., S. Vassileva, and M. Natov. 2004. *J. App. Polym. Sci.* 90: 2734-2739.
- Wool, R. and X-S. Sun, Eds. 2005. *Bio-based Polymers and Composites*. Elsevier Academic Press. ISBN 0127639527.
- Wu, C-S. 2004. *J. App. Polym. Sci.* 94: 1000-1006.
www.me.gatech.edu/jonathan.colton/me4793/natfiber.pdf.
- Zaini, M.J., M.Y.A. Fuad, Z. Ismail, and M.S. Mustafah. 1996. *Polym. Int.* 40(1): 51-55.
- Zuiderduin, W.C.J., C. Westzaan, J. Huetink, and R.J. Gaymans. 2003. *Polymer*. 44: 261-275.

9th International Conference on Wood & Biofiber Plastic Composites

May 21-23, 2007

*Monona Terrace Community & Convention Center
Madison, Wisconsin, USA*

The conference was hosted by the USDA Forest Service,
Forest Products Laboratory and Forest Products Society,
In cooperation with the Canadian Natural Composites Council,
IUFRO Composites & Reconstituted Products Division,
Luleå University of Technology, University of Tennessee's Forest
Products Center, and University of Toronto's Faculty of Forestry
and Centre for Biocomposites & Biomaterials Processing.



Forest Products Society
2801 Marshall Court
Madison, WI 53705-2295
phone: 608-231-1361
fax: 608-231-2152
www.forestprod.org

The opinions expressed are those of the authors and do not necessarily represent those of the USDA Forest Service or the Forest Products Society.

Copyright © 2007 by the Forest Products Society.
Proceedings No. 7224
ISBN-892529-50-5

All rights reserved. No part of this publication may be reproduced, stored in a retrieval system, or transmitted, in any form or by any means, electronic, mechanical, photocopying, recording, or otherwise, without prior written permission of the copyright owner. Individual readers and nonprofit libraries are permitted to make fair use of this material such as to copy an article for use in teaching or research. To reproduce single or multiple copies of figures, tables, excerpts, or entire articles requires permission from the Forest Products Society and may require permission from one of the original authors.

Printed in the United States of America.

0711300